Gamma-ray Irradiation Effects on InAs/GaSb-based nBn IR Detector

Vincent M. Cowan[*1], *Christian P. Morath*[1], *Seth M. Swift*[1], *Stephen Myers*[2], *Nutan Gautam*[2], *Sanjay Krishna*[2]
[1]Air Force Research Laboratory --Space Vehicles Directorate, 3550 Aberdeen Ave SE, Kirtland AFB, NM 87117, USA;
[2]Center for High Technology Materials, University of New Mexico, Albuquerque, NM 87106, USA

ABSTRACT

IR detectors operated in a space environment are subjected to a variety of radiation effects while required to have very low noise performance. When properly passivated, conventional mercury cadmium telluride (MCT)–based infrared detectors have been shown to perform well in space environments. However, the inherent manufacturing difficulties associated with the growth of MCT has resulted in a research thrust into alternative detector technologies, specifically type-II Strained Layer Superlattice (SLS) infrared detectors. Theory predicts that SLS-based detector technologies have the potential of offering several advantages over MCT detectors including lower dark currents and higher operating temperatures. Experimentally, however, it has been found that both p-on-n and n-on-p SLS detectors have larger dark current densities than MCT-based detectors. An emerging detector architecture, complementary to SLS-technology and hence forth referred to here as *nBn*, mitigates this issue via a uni-polar barrier design which effectively blocks majority carrier conduction thereby reducing dark current to more acceptable levels.

Little work has been done to characterize nBn IR detectors tolerance to radiation effects. Here, the effects of gamma-ray radiation on an nBn SLS detector are considered. The nBn IR detector under test was grown by solid source molecular beam epitaxy and is composed of an InAs/GaSb SLS absorber (*n*) and contact (*n*) and an $Al_xGa_{1-x}Sb$ barrier (*B*). The radiation effects on the detector are characterized by dark current density measurements as a function of bias, device perimeter-to-area ratio and total ionizing dose (TID).

Keywords: nBn, SLS, InAs/GaSb, total ionizing dose, TID, superlattice, gamma irradiation, infrared

1. INTRODUCTION

1.1 Motivation

This paper presents recent experimental findings of electrical and optical characterization of an InAs/GaSb strained-layer superlattice (SLS) infrared (IR) detector utilizing a nBn design in a gamma radiation environment. Optical and electrical characterizations of a similar nBn detector were previously reported.[1] Here, the analysis regarding the characterizations reported in this experiment is focused on the dark current surface effects, total ionizing dose (TID), and gamma-induced transient measurements. In exploring the utility of nBn detectors for potential space-based imaging applications, it's paramount to understand the effects of total dose effects for this detector architecture.

1.2 IR Detector Technologies for Space Applications

Focal plane arrays (FPAs) developed for imaging applications in a space environment are meticulously characterized to evaluate their sensitivity, uniformity, operability, and radiation hardness. Pursuit of these performance metrics for alternative materials to HgCdTe are intended to enhance technology development in multispectral sensors, higher pixel

* vincent.cowan@kirtland.af.mil

Quantum Sensing and Nanophotonic Devices VIII, edited by Manijeh Razeghi, Rengarajan Sudharsanan, Gail J. Brown, Proc. of SPIE Vol. 7945, 79451S · © 2011 SPIE · CCC code: 0277-786X/11/$18 · doi: 10.1117/12.873413

Report Documentation Page

Form Approved
OMB No. 0704-0188

1. REPORT DATE	2. REPORT TYPE	3. DATES COVERED
2011		**00-00-2011 to 00-00-2011**

4. TITLE AND SUBTITLE	5a. CONTRACT NUMBER
Gamma-ray Irradiation Effects on InAs/GaSb-based nBn IR Detector	5b. GRANT NUMBER
	5c. PROGRAM ELEMENT NUMBER
6. AUTHOR(S)	5d. PROJECT NUMBER
	5e. TASK NUMBER
	5f. WORK UNIT NUMBER
7. PERFORMING ORGANIZATION NAME(S) AND ADDRESS(ES) **Air Force Research Laboratory,Space Vehicles Directorate,3550 Aberdeen Ave SE,Kirtland AFB,NM,87117**	8. PERFORMING ORGANIZATION REPORT NUMBER
9. SPONSORING/MONITORING AGENCY NAME(S) AND ADDRESS(ES)	10. SPONSOR/MONITOR'S ACRONYM(S)
	11. SPONSOR/MONITOR'S REPORT NUMBER(S)

12. DISTRIBUTION/AVAILABILITY STATEMENT
Approved for public release; distribution unlimited

13. SUPPLEMENTARY NOTES

14. ABSTRACT

IR detectors operated in a space environment are subjected to a variety of radiation effects while required to have very low noise performance. When properly passivated, conventional mercury cadmium telluride (MCT)?based infrared detectors have been shown to perform well in space environments. However, the inherent manufacturing difficulties associated with the growth of MCT has resulted in a research thrust into alternative detector technologies, specifically type-II Strained Layer Superlattice (SLS) infrared detectors. Theory predicts that SLS-based detector technologies have the potential of offering several advantages over MCT detectors including lower dark currents and higher operating temperatures. Experimentally, however, it has been found that both p-on-n and n-on-p SLS detectors have larger dark current densities than MCT-based detectors. An emerging detector architecture, complementary to SLS-technology and hence forth referred to here as nBn, mitigates this issue via a uni-polar barrier design which effectively blocks majority carrier conduction thereby reducing dark current to more acceptable levels. Little work has been done to characterize nBn IR detectors tolerance to radiation effects. Here, the effects of gamma-ray radiation on an nBn SLS detector are considered. The nBn IR detector under test was grown by solid source molecular beam epitaxy and is composed of an InAs/GaSb SLS absorber (n) and contact (n) and an AlxGa1-xSb barrier (B). The radiation effects on the detector are characterized by dark current density measurements as a function of bias, device perimeter-to-area ratio and total ionizing dose (TID).

15. SUBJECT TERMS

16. SECURITY CLASSIFICATION OF:			17. LIMITATION OF ABSTRACT	18. NUMBER OF PAGES	19a. NAME OF RESPONSIBLE PERSON
a. REPORT	b. ABSTRACT	c. THIS PAGE			
unclassified	**unclassified**	**unclassified**	**Same as Report (SAR)**	**8**	

sensitivities, larger array formats with higher pixel densities, higher operating temperatures, simplified manufacturing techniques, and reduced costs. Specific to space applications is radiation hardness, which is required to mitigate detrimental effects on IR detectors exposed to radiation from energetic charged particles held in place by the earth's magnetic field or compressed by solar winds. Detector technologies that effectively operate in the harsh radiation environment of space afford greater flexibility in orbit selection, technical applications, and system sustainability.[2]

For IR detectors operating in the mid-wave (MWIR) and long-wave (LWIR), InAs/GaSb type-II SLS are the only material known to have a theoretically predicted higher performance than HgCdTe.[3, 4] Among the primary limiters of HgCdTe performance is the Auger lifetime, which is calculated to be much longer for SLS materials. This indicates a SLS detector would be less constrained by noise from dark currents at the same wavelengths and operating temperatures as a HgCdTe detector with the same absorption characteristics.[5] While significant progress is being made to reduce the dark current measured in SLS detectors comparable to, or lower than, HgCdTe detectors, this has not yet been demonstrated. However, the degraded performance may not be limited by the Auger lifetime, but rather the noise due to generation–recombination (G–R) and trap-assisted tunneling processes in the material's depletion region.[6]

Research pursuits in type-II SLS detectors utilizing the nBn architecture are showing potential in reducing the dark current. This nBn detector operates by diffusion of the photo-generated minority hole carriers. Composed of two SLS n-type layers, the first n-type layer acts as a narrow band gap semiconductor to absorb incoming photons. Separating this absorption layer from the other n-type contact layer is a thin layer of wider-band gap GaSb "barrier" material, which is engineered to have a large conduction band offset to block electron currents, and zero valence band offset to permit hole currents. Thus, the barrier material permits the photo-generated electron-hole pairs generated in the n-type narrow band gap absorber layer to be collected.[7] Furthermore, in the nBn architecture the depletion region is restricted to the large bandgap barrier material layer, which results in a drastically reduced Shockley-Read-Hall (SRH) generation component. This enables background-limited infrared photodetection (BLIP) performance at higher operating temperatures than typical InAs-based MWIR devices.[8, 9]

1.3 Radiation Tolerance of InAs/GaSb-based nBn Detectors

Concerning space-based applications, characterizations of type-II SLS detectors operating in a radiation filled environment have not been widely reported. To the authors' knowledge, there are no reports of radiation tolerance studies for IR detectors with the nBn architecture. The Naval Research Laboratory has reported that there is little degradation below 1 Mrad(Si) from incremental proton fluences of 1 MeV on first-generation antimony-based type-II SLS samples.[10] This provides a good indication regarding the radiation tolerances of these materials without considering other performance metrics. Further reporting on radiation damage for more advanced SLS architectures operating in the LWIR also shows potential for space applications.[11]

The nBn IR detector under test, illustrated in Figure 1, is composed of an InAs/GaSb SLS absorber (*n*) and contacts (*n*) with an $Al_xGa_{1-x}Sb$ barrier (*B*) grown by solid source molecular beam epitaxy (MBE). This particular detector architecture was developed by the Center for High Technology Materials (CHTM) at the University of New Mexico. Analysis of the optical and electrical characterization in a gamma radiation environment provides indicators of potential detector degradation from a space standpoint. Degradation from the gamma irradiation dose can result from the accumulation of trapped electrons that alter the detector's electrical properties and ultimately can lead to functional failure. Single event latchup is caused by energetic particles that turn on parasitic elements, creating high current paths, and rendering circuits inoperable.[12]

The scope of this paper is to present the results from a recent characterization of an nBn detector's tolerance to TID. The gamma radiation that was used for this study was produced using the Air Force Research Laboratories (AFRL) Cobalt-60 source located at Kirtland Air Force Base.

2. EXPERIMENTAL SETUP

2.1 Device Fabrication

The device was grown at CHTM using solid source molecular beam epitaxy in a VG-80 system. Specific details on the growth methods have been previously reported Once grown, the material was processed using dry etching techniques and conventional optical photolithography. This resulted in the formation of 410µm by 410µm single-pixel detectors and square diodes with sides ranging in size from 400-30µm. The nBn detector did not receive an antireflection coating. The layout of the nBn evaluation chip is illustrated in Figure 1. Both the common back plane and the top contacts of the individual detectors were wire-bonded to a 68 pin leadless chip carrier (LCC).

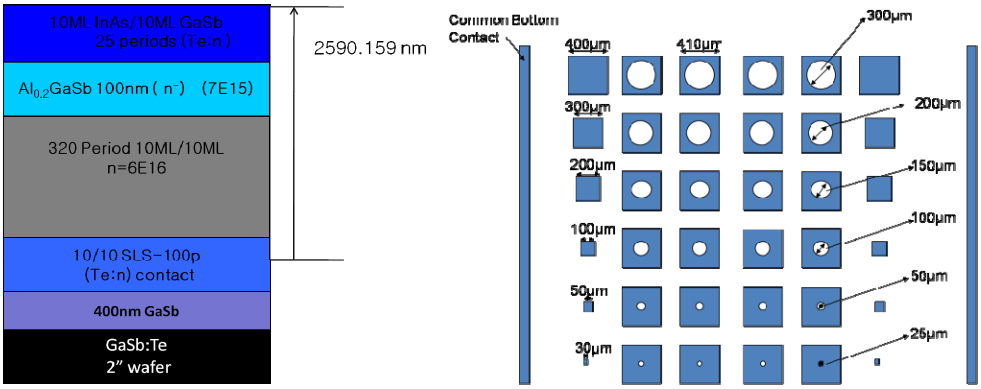

Figure 1. Schematic of the nBn wafer structure (left), and test chip layout (right). Devices on left (right) hand side of chip layout are shallow (deep) etched.

The orientation in which bias is applied across the detector is opposite to that of a conventional PIN photodiode; here, the tops of each individual detector were grounded while the bias was applied to the common back plane. For this experiment eight different devices were measured including both shallow and deep-etched 410 µm x 410 µm nBn single element detectors with 200 µm diameter active area, and 400 µm, 300 um, 200 um square variable area diodes. The devices were characterized from electrical and optical standpoint as a function of TID using the test bed described in the section to follow.

2.2 Dosimetry

Dosimetry was performed by placing a dosimeter that measures dose rate in the plane inside the dewar which the detector under test would sit. The dewar was configured such that all of the shielding that was needed to conduct the nBn radiation tolerance study was in place while the dosimetry was performed. The distance between the plane in which the dosimeter was located and where the cobalt source would be located, once raised, was recorded. The Cobalt-60 source was then raised for a fixed period of time and the dose rate was recorded independently three times. This procedure was repeated for a total of four different distances between the dosimeter and the source and the results were plotted on a log-log scale, as shown in Figure 2.

Using this data a mathematical relationship was determined that describes the dose rate as a function of the distance between part under test and the Cobalt-60 source. Using that relationship the appropriate exposure times for the remainder of the work presented was determined.

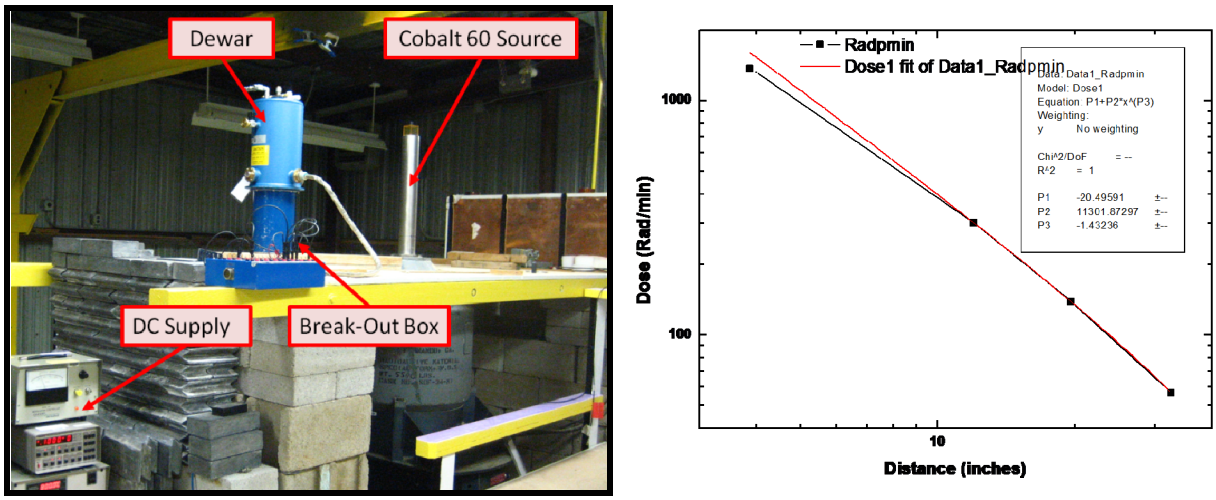

Figure 2. Dose rate (Rad/min) as a function of distance between part under test and Cobalt-60 source.

2.3 Electrical & Optical Test Bed

Figure 3 shows the mobile test bed that was assembled to characterize both the optical and electrical properties of the infrared detector at the radiation facility. The LCC mounted nBn detector chip used here was secured to the cold-finger of a pour-filled dewar capable of reaching liquid helium (LHe) temperatures. Both the inner and outer flasks of the dewar were filled with liquid nitrogen (LN2).

A metal shield with a 1 mm aperture pinhole was placed around the detector and cooled to 77 K. Dark currents were measured with the pinhole configuration as just described and with the device completely shuttered from background light and an insignificant change was observed. The dark current of the device was then measured using a Keithley model 236 source-measure unit. Voltage ranging from -1 V to 2 V was applied across the detector while simultaneously measuring the current through the device. The positive lead of the instrument was attached to the common back plane of the device while the negative lead was attached to the top of the individual diodes and detector pixels. Once the dark current was measured for each diode the process was repeated for total ionizing doses ranging up to 200 krads (Si).

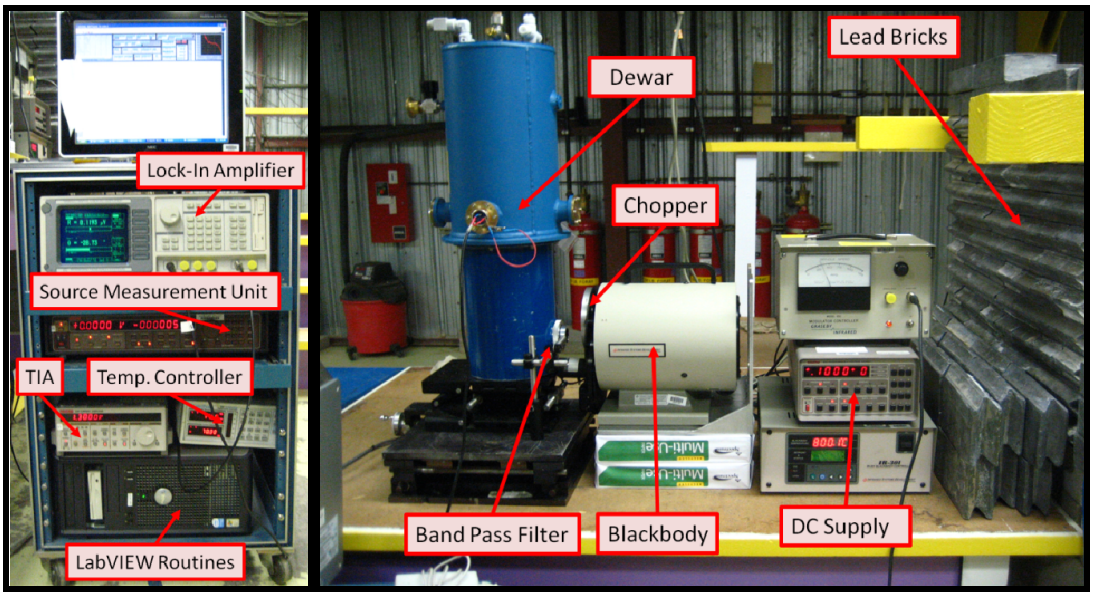

Figure 3. Mobile Electrical Test Bed (left) & optical characterization test bed (right) for the nBn detector.

The spectral response of the detector was measured with a Nicolet 670 Fourier transform infrared (FTIR) spectrometer using a Keithly 428 trans-impedance amplifier (TIA) to bias the nBn detector under test to 100 mV. Similarly, the spectral response of an infrared band pass filter was measured to have cut-on and cut-off wavelengths of 3.6 µm and 4.2 µm, respectively.

A blackbody source spectral profile was confined to the waveband of the band pass filter and then modulated using an optical chopper. This signal fills the field of view of the nBn IR detector, which was kept at an operating temperature of 77 K inside the dewar. The optical geometry of this test bed was such that a cold 1mm diameter limiting aperture was located 50 cm in front of the device. A Keithly 428 TIA was used to provide a bias across the nBn detector and convert the current through the detector to an amplified voltage level adequate to drive a Stanford Research System SR850 lock-in amplifier

Using these measurable quantities, the local (3.6µm - 4.2µm) peak responsivity of the nBn IR detector was determined. Peak responsivity was calculated using the following equation:

$$R_{peak} = \frac{I_{ph}}{MF \cdot A_D \cdot \Omega \cdot \left(\frac{\pi}{\pi}\right) \cdot \int_{\lambda_1}^{\lambda_2} R^1(\lambda) \left[M_b(\lambda, T_{BB}) - M_c(\lambda, T_a)\right] T_w(\lambda) T_f(\lambda) d\lambda} \quad (1)$$

where I_{ph} is the current measured through the detector, MF is the modulation factor of the optical chopper, A_D is the area of the detector, Ω is the projected solid angle of incident radiation on the detector, R^1 is the relative spectral response, M_b is the spectral exitance of the black body source, M_c is the spectral exitance of the chopper wheel, T_f is the transmission of the band pass filter, T_{BB} is the blackbody temperature, T_a is the ambient temperature, and T_w is the transmission of the window on the front of the dewar. Data acquisition and post processing took place using an automated custom LabVIEW program developed by AFRL.

A bias of 100 mV was applied across all of the detectors using a break box during radiation exposure to simulate the conditions that would be present if the detector were used on a platform operated in a radiation environment. The following section will present the electrical and optical characterization results for the nBn detector using the characterization test bed described above.

3. RESULTS & DISCUSSION

3.1 nBn electrical characterization results

The dark current density of the 200 µm shallow etched nBn detector operated at 77 K as a function of voltage and TID, is shown in Figure 4. One can see that a small, but measurable change on the order of 5 % was observed as the TID was increased up to 200 kRad(Si). Measurement noise, on the order of .1 %, was also present as shown in the data below. Similar behavior was observed for the deep etched detector and the variable area diodes. These results suggest the nBn detector is tolerant of TID and that surface currents, which TID typically enhances due to electron trapping, may have minimal contribution to overall dark current density.

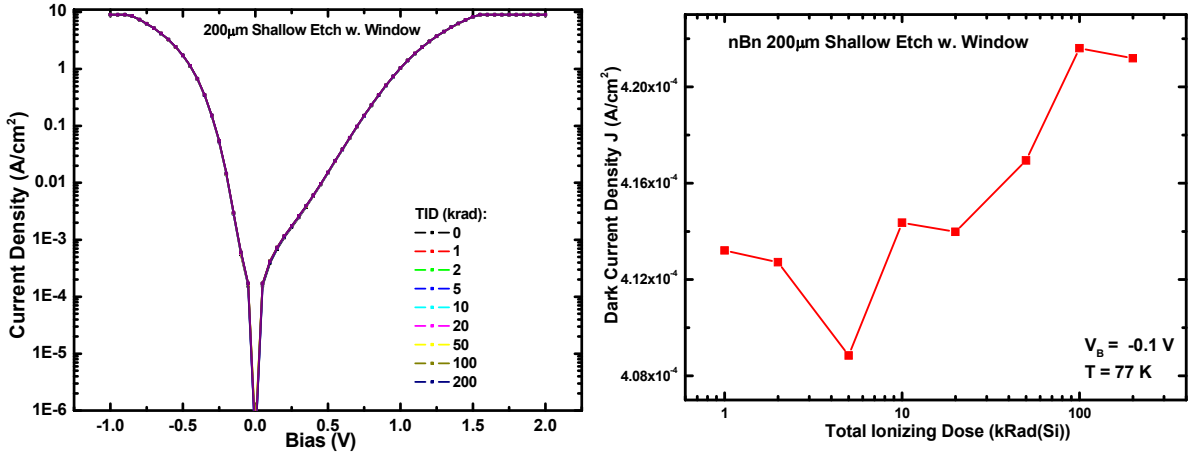

Figure 4. Dark current densities as a function of bias (left) and TID with fixed applied bias equal to 100 mV (right) for a 200 um shallow etched device at T = 77 K.

The dark current measurements at various biases for the variable area diodes were also compiled as a function of the area-to-perimeter ratios. This was done for both the deep and shallow etch devices, as shown in Figure 5. Examining these results, first and foremost, we see there is again only a small increase in dark current density, at most bias voltages, for TID up to 200 kRad(Si), suggesting a strong tolerance. Secondly, as expected dark current density increases with increasing bias for either polarity and with a less rapid increase for positive bias, as is typically observed due to the presence of the barrier.

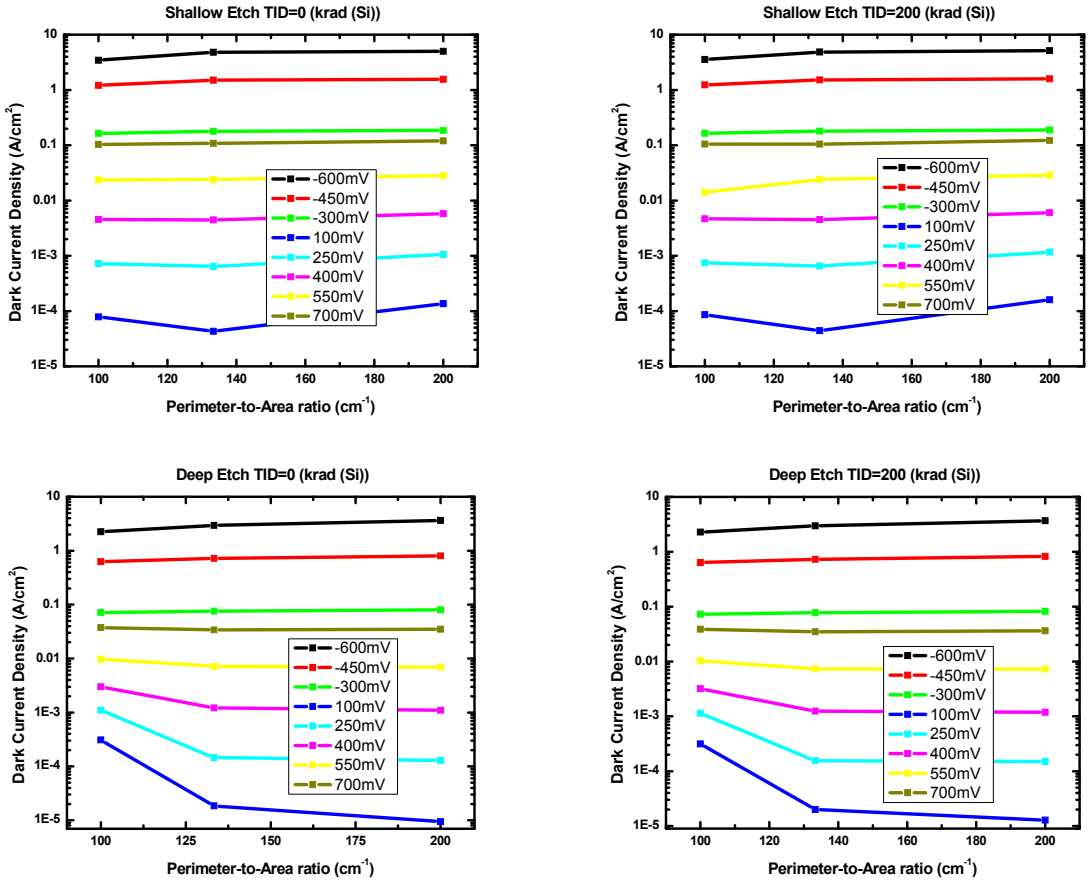

Figure 5. Dark current densities as a function of perimeter-to-area ratio for shallow (top) and deep (bottom) etched devices at TID = 0 (left) and TID = 200 krad (Si) (right).

Finally, these results also suggest that overall this nBn-SLS detector does not appear to suffer from large surface currents that often plague detector technologies, especially at the onset of their development. Rather, a closer look at the plots in Figure 5 reveals different behaviors depending on the bias polarity. As bias voltage was made more negative the results begin to show increasing dark current density as device sized decreased (larger perimeter-to-area ratio) appearing to suggest a small surface current component arises. However, at positive bias voltages the results indicate a decrease in dark current density with decreasing device size. The amount of change becomes smaller as the bias is made more positive until the curve has roughly zero slope at V = 700 mV. The source of this unexpected negative slope for positive bias voltages and the overall dependence on polarity is not completely understood. It may reflect a lack of overall device uniformity or not testing large enough perimeter-to-area ratios. However, it may also indicate some kind of built-in surface voltage, due to an n-type surface layer arising in the barrier layer. Further testing is thus required to understand fundamentally what is occurring on the sidewalls of the devices.

3.2 nBn optical characterization results

This section discusses the optical characteristics of the nBn IR detector. The overall spectral profile of the nBn detector at an operation temperature of 77 K and biased at 100 mV is shown in Figure 6. Likewise, the transmission profile of the mid-IR bandpass filter used to measure the responsivity is also shown in Figure 6. A bandpass filter with a known spectral response ensures that only a known amount of infrared light is incident on the detector.

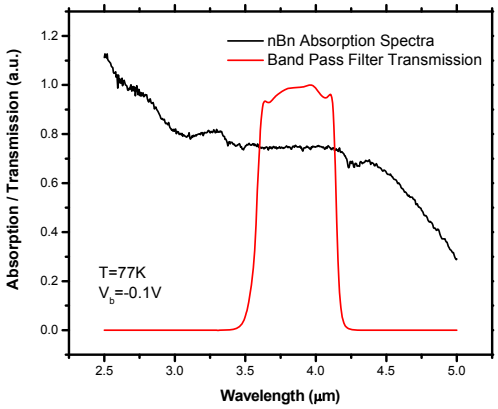

Figure 6. Absorption profile of nBn detector and transmission of band pass filter.

Inserting measured quantities into equation (1) presented in section 2.3, the peak responsivity across the 3.6 μm - 4.2μm band of the nBn detector was calculated as a function of the bias applied across the detector. It should be noted that absorption of the nBn detector is very flat over the range of the bandpass filter.

With 100 mV applied across the detector and the peak responsivity was measured to be 296 mA/W. The irradiance light level from the blackbody source that was incident on the detector was estimated to be 9.82 x 10^{10} photons/sec cm^2. The responsivity of both the shallow and deep etched detectors were measured for each order of magnitude change in TID, namely 0, 1, 10, and 100kRad(Si). As expected, no appreciable change in the responsivity of the detectors was observed as TID increased, as shown in Figure 7.

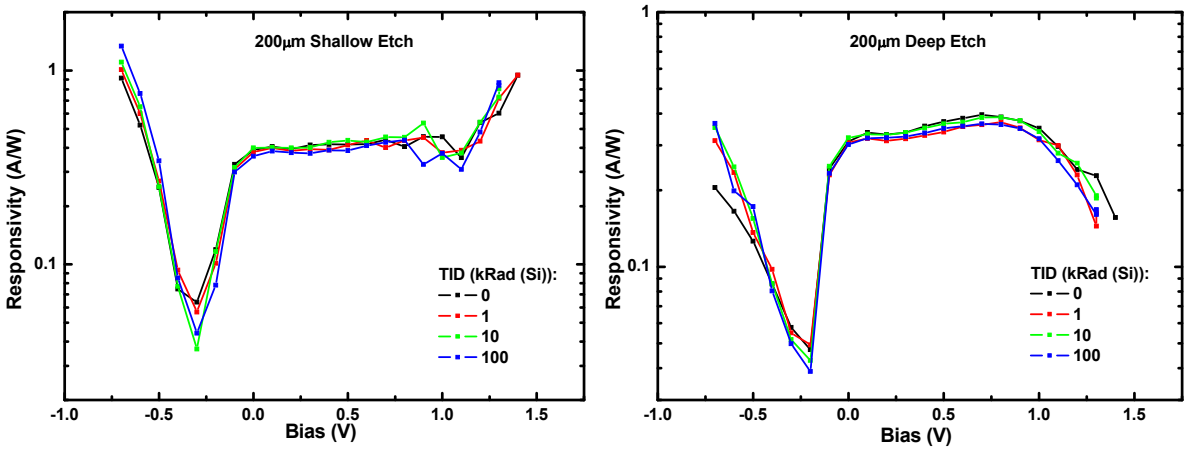

Figure 7. Peak responsivity (3.6μm – 4.2μm range) as a function of bias, shallow etched (left), deep etched (right).

A logical operational bias for this detector occurs at 0.1 V which corresponds to a dark current density of 420 μA/cm^2 and a responsivity of 296 mA/W across the 3.6 μm - 4.2μm band.

4. CONCLUSION

In conclusion, to the best of our knowledge this is the first time TID radiation tolerance of a SLS-based nBn architecture infrared detector has been measured. This new detector technology has shown no significant change in the dark current density up to a TID of 200 kRad(Si). It was also observed that the dark current density dependence on perimeter-to-area ratio was a function of bias polarity, although overall surface current effects did not appear significant. Further investigation of surface current effects using smaller devices is thus required. Finally, as expected no significant degradation in the optical responsivity was observed as a function of TID. Future work will also focus on effects that proton radiation have on the bulk of the nBn detector.

5. ACKNOWLEDGEMENTS

The authors would like to acknowledge Dr John Hubbs and his team from Infrared Radiation Effects Laboratory for their guidance. Likewise work was possible with the funding awarded under AFOSR Contract No. FA9550-09-1-0231 and AFRL Contract No. FA9453-07-C-0171.

6. REFERENCES

[1] V. M. Cowan, C. P. Morath, S. M. Swift, P. D. LeVan, S. Myers, E. Plis, S. Krishna, "Electrical and Optical Characterization of InAs/GaSb-based nBn IR Detector," Proc. SPIE, Vol. 7780, 778006 (2010).

[2] N. Sramek, "Radiation Hardened Electronics for Space Systems," June 12, 2001.

[3] G. A. Sai-Halasz, R. Tsu, and L. Esaki, Appl. Phys. Lett. 30, 651 (1977).

[4] D. L. Smith and C. Mailhiot, J. Appl. Phys. 62, 2545 (1987).

[5] D. R. Rhiger, "Performance Comparison of LWIR Type-II Superlattice Devices with HgCdTe," 2010 U.S. Workshop on the Physics and Chemistry of II-VI Materials, Extended Abstracts, 25, (2010).

[6] E. Plis, J. B. Rodriguez, G. Balakrishnan, Y. D. Sharma, H. S. Kim, T. Rotter, S. Krishna, "Mid-infrared InAs/GaSb strained layer superlattice detectors with nBn design grown on a GaAs substrate," Semiconductor Science and Technology, 25 085010 (2010).

[7] H. S. Kim, G. D. Bishop, J. B. Rodriguez, Y. Sharma, E. Plis, L. R. Dawson, and S. Krishna, "Suppressed Surface Leakage Current Using nBn Infrared Detector Based on Type II InAs/GaSb Strain Layer Superlattices," The 20th Annual Meeting of the IEEE Lasers and Electro-Optics Society, LEOS (2007).

[8] G. Bishop, "InAs/Ga(In)Sb Superlattice Based Infrared Detectors using nBn Design," Masters Thesis, University of New Mexico pg 25 (2008).

[9] S. Maimon and G. W. Wicks, Appl. Phys. Lett. 89, 151109 (2006).

[10] B. D. Weaver, E. H. Aifer, "Radiation Effects in Type-Two Antimonide Superlattice Infrared Detectors," IEEE Transactions on Nuclear Science, Vol. 56, No. 6, 6, December (2009).

[11] E.M. Jackson, E.H. Aifer, C.L. Canedy, J.A. Nolde, C.D. Cress, B.D. Weaver, I. Vurgaftman, J.H. Warner, J.R. Meyer, J.G. Tischler, S.A. Shaw, and C.R. Dedianous, "Radiation damage in type-II superlattice infrared detectors," Journal of Electronic Materials, Vol. 39, No. 7, (2010).

[12] N. Sramek, "Radiation Hardened Electronics for Space Systems" The Aerospace Corporation, available at ewh.ieee.org/r6/lac/csspsvts/briefings/sramek.pdf, June 12, (2001).